

Article

Influences of Cosolvents and Antifreeze Additives Derived from Glycerol through Esterification on Fuel Properties of Biodiesel

Cherng-Yuan Lin *  and Yun-Chih Chen

Department of Marine Engineering, National Taiwan Ocean University, Keelung 20224, Taiwan; cyzclare@gmail.com

* Correspondence: lin7108@ntou.edu.tw; Tel.: +886-2-24622307

Abstract: Bioglycerol is a major by-product of the biodiesel manufacturing process. Various chemical derivatives from bioglycerol would enhance its economic value. An antifreeze of glycerine acetate was chemically converted from an esterification reaction of bioglycerol with acetic acid. The photocatalyst $\text{TiO}_2/\text{SO}_4^{2-}$ irradiated with ultraviolet light assisted the chemical conversion reaction. The molar ratio of acetic acid/bioglycerol was varied to obtain the optimum composition of the derived antifreeze product. Different cosolvents were considered to enhance the homogeneous extent between the antifreeze of glycerine acetate and biodiesel, and thus, the anti-freezing effect. The cosolvent/glycerine acetate, at various volumetric ratios from 0 to 0.25 vol.%, was blended into a commercial biodiesel. After 5 vol.% antifreeze of the glycerine acetate/cosolvent mixture of the biodiesel was added to the commercial biodiesel, the fuel properties of the biodiesel were analyzed. The effects of the cosolvent types and the blended volumetric ratio of cosolvent to the antifreeze of glycerine acetate on the fuel properties of the commercial biodiesel were analyzed to determine the optimum cosolvent type and volumetric composition of the cosolvent/glycerine acetate. The experimental results show that the antifreeze of glycerine acetate produced from the reaction of acetic acid/glycerol at a molar ratio equal to 8 under UV-light irradiation appeared to have the lowest freezing point. The UV-light irradiation on the $\text{TiO}_2/\text{SO}_4^{2-}$ catalyst also caused higher triacylglycerol (TAG) and diacylglycerol (DAG) and lower monoacylglycerol (MAG) formation. In addition, the low-temperature fluidity was the most excellent when the volumetric percentage of the methanol/glycerine acetate was equal to 0.25 vol.%, at which the cold filter plugging point (CFPP) of the biodiesel was reduced from 3 °C for the neat biodiesel to −2 °C for the biodiesel blended with the mixture. In contrast, the effect of adding the antifreeze on the CFPP of the biodiesel was inferior; it was reduced from 3 °C for the neat biodiesel to 1 °C for the biodiesel when butanol cosolvent was added. The increase in the volumetric ratio of cosolvent/antifreeze increased the acid value and cetane index while it decreased the kinematic viscosity and CFPP. The heating value was observed to increase for butanol while decreasing for methanol with the increase in the volumetric ratio of cosolvent/antifreeze. In comparison to butanol, the cosolvent methanol caused a higher cetane index and acid value but a lower kinematic viscosity, heating value, and CFPP of the blended commercial biodiesel.

Keywords: fuel properties; cold filter plugging point; biodiesel; cetane index; kinematic viscosity



Citation: Lin, C.-Y.; Chen, Y.-C. Influences of Cosolvents and Antifreeze Additives Derived from Glycerol through Esterification on Fuel Properties of Biodiesel. *Processes* **2024**, *12*, 419. <https://doi.org/10.3390/pr12020419>

Academic Editor: Antoni Sanchez

Received: 31 January 2024

Revised: 14 February 2024

Accepted: 16 February 2024

Published: 19 February 2024



Copyright: © 2024 by the authors. Licensee MDPI, Basel, Switzerland. This article is an open access article distributed under the terms and conditions of the Creative Commons Attribution (CC BY) license (<https://creativecommons.org/licenses/by/4.0/>).

1. Introduction

Biodiesel is produced from the transesterification reaction of vegetable oil, animal fats, or microalgae with straight-chained alcohols, particularly methanol, under the catalytic effects of strong alkaline catalysts, such as sodium methoxide, sodium hydroxide, or potassium hydroxide, or strong acid catalysts, like sulfuric acid or hydrochloric acid [1]. Biodiesel is an excellent alternative to petroleum-derived diesel primarily due to its relatively low elemental carbon, superior combustion efficiency, low toxic gas emission, biodegradability, environmentally friendly fuel properties, etc. [2]. Glycerol, or glycerin, is a colorless,

odorless, viscous liquid with a boiling point of 290 °C, a molecular weight of 92.09, and an absolute viscosity of 1.5 Pa-s [3]. Glycerol has three hydroxyl groups responsible for its water solubility and hygroscopic properties. Glycerol is mainly used to formulate cosmetics, pharmaceuticals, and medications to improve their smoothness. Bioglycerol is a by-product of biodiesel production, which contains unreacted soap, catalysts, and excess alcohol, so the product's value is low. The purification process for glycerol is frequently rather costly. The purification of crude glycerin requires the removal of methanol and free fatty acids, neutralizing, and decolorizing. Applying an organic polymer membrane, ion exchange resin, electro-osmosis, vacuum distillation, etc., is then involved in attaining high-purity glycerin [4]. Due to fast growth in the biodiesel manufacturing industry, the amount of bioglycerol is increasing steadily. In 2025, crude glycerol will amount to 300 million tons, while less than only 5 million tons of glycerol will be consumed annually for industrial purposes [5]. The significant excess of bioglycerol production from the biodiesel manufacturing process results in considerably low economic value. Bioglycerol can also be chemically converted to produce various derivative products, such as propionic acid, glycerol carbonate n-butanol, dioxane, dioxalane, hydrogen, etc., with the assistance of some adequate catalysts [6]. The products from converted bioglycerol can be widely applied in the fuel, food, and textile sectors, significantly increasing the entire economic value of biodiesel and glycerol-derived products. Using competitive catalysts to synthesize high-value products from bioglycerol is crucial for reaching this objective.

Titanium dioxide (TiO_2) is a versatile compound that can be used in many ways, especially in hydrogen production from the chemical conversion of hydrocarbons, in the cleanup of polluted environments, and in the treatment of wastewater under the catalyzing effects of TiO_2 , which acts as an efficient photocatalyst [7]. Under irradiation of ultraviolet (UV) light, glycerol can more efficiently react with acetic acid to produce glycerine acetate. The heterogeneous strong acid catalyst $\text{TiO}_2/\text{SO}_4^{2-}$ is prepared by leaching TiO_2 powder of nanometer (nm) size, immersing it in dilute sulfuric acid, and then filtering, drying, and forging it [8]. Heterogeneous strong acid catalysts frequently have the dominant advantages of superior mechanical properties, thermal stability, and enhancing effects for chemical reactions compared to traditional homogeneous acid catalysts [9].

One of the major disadvantages of biodiesel is its inferior fluidity in cold regions or frigid winters, which might deteriorate drivability or even shut down the internal combustion engines of vehicles. Its poor low-temperature fluidity significantly hinders biodiesel's wide application in the global fuel market. Blending adequate antifreeze additives into biodiesel could improve its fluidity properties and increase its economic value [10]. Moreover, the huge amount of bioglycerol made from the biodiesel production process causes its low monetary value. Glycerine acetate compounds are primarily composed of a mixture of triacylglycerols (TAGs), diacylglycerols (DAGs), and monoacylglycerols (MAGs), which are chemically converted from the esterification of glycerol with acetic acid, assisted by a $\text{TiO}_2/\text{SO}_4^{2-}$ photocatalyst irradiated with ultraviolet (UV) light. The exact compositions of glycerine acetate produced through this reaction can be analyzed by gas chromatography.

The advanced development of antifreeze derived from bioglycerol could exploit its application scope and increase the competitive extent of the entire biodiesel product chain. Hence, a comprehensive evaluation of the production methods for glycerol-derived additives is an important step in developing promising technologies for glycerol conversion. In addition, more studies are needed to investigate the effects of glycerol-derived additives on the improvement of biodiesel's fuel characteristics [11]. Most previous relevant studies only focused on the characteristics analysis of the catalysts used for bioglycerol conversion [12]. Moreover, the effects of the addition of a promising antifreeze produced from the chemical conversion of glycerol to liquid fuels on fuel characteristics have yet to be comprehensively investigated to improve their properties such as the kinematic viscosity and cetane index, and particularly, their low-temperature fluidity. In this experiment, the effects of the cosolvent type and the volumetric ratio of cosolvent/glycerine acetate on the fuel properties of a blended biodiesel mixture were considered. After the antifreeze of glycerine acetate was

produced, it was blended with methanol or butanol cosolvent to form an antifreeze additive mixture. The antifreeze additive of glycerine acetate and biodiesel are not well miscible with each other. An adequate cosolvent would effectively increase their contacting interface and form a single homogeneous phase so that the antifreeze could intimately mix with the biodiesel to expand its anti-freezing effect. Different cosolvents were considered to enhance the homogeneous extent of the antifreeze of glycerine acetate and biodiesel. Alcohols with various carbon chains have been used as cosolvents to improve the transesterification of triglycerides. Methanol is the most frequently used one among the available alcohols. Butanol and pentanol have also proven their cosolvent activity in enhancing the miscible extents of the compounds of reactant mixtures [13,14]. In this study, methanol and butanol were considered as cosolvents to evaluate their effects on improving the anti-freezing property of biodiesel. The physical and chemical properties of the antifreeze additive of glycerine acetate derived from bioglycerol have not yet been quantitatively investigated. The effects of alcohol cosolvents on improving the fuel properties of biodiesel have not yet been thoroughly evaluated. The fuel properties of biodiesel before and after adding various proportions of a cosolvent and antifreeze additive have not been comprehensively analyzed and compared, particularly the significant properties of the cold filter plugging point (CFPP) and kinematic viscosity. Hence, various volumetric proportions of the cosolvent and glycerine acetate were prepared. The cosolvents/glycerine acetate mixture at a volumetric ratio of 5 vol.% of the biodiesel was then blended into a commercial biodiesel. The properties of the freezing point, acid value, cetane index, kinematic viscosity, and the low-temperature fuel fluidity of the biodiesel blended with the cosolvent/antifreeze of the glycerine acetate additive were analyzed. The optimum reaction conditions for the antifreeze additive produced from bioglycerol and the adequate volumetric ratio of the cosolvent/glycerine acetate to improve the biodiesel properties were determined.

2. Experimental Details

A heterogeneous strong acid photocatalyst, $\text{TiO}_2/\text{SO}_4^{2-}$, was prepared to catalyze the chemical conversion reaction of bioglycerol, leading to the formation of an antifreeze of glycerine acetate. The fuel characteristics of the antifreeze were analyzed to improve the reaction conditions for its production. An adequate amount of either methanol or butanol cosolvent was blended with the glycerides before the mixture was added to the biodiesel to act as an antifreeze. The fuel properties of the biodiesel after being added to the antifreeze were analyzed afterward.

2.1. Preparing the Antifreeze from Bioglycerol

Bioglycerol, a by-product of biodiesel production processes, was used to perform an esterification reaction with acetic acid. The physical properties of the glycerol used in this study are shown in Table 1 [15]. A solid-state strong acid photocatalyst, $\text{TiO}_2/\text{SO}_4^{2-}$, was prepared by immersing TiO_2 powder in a sulfuric acid solution and then filtered, baked for 4 hrs at 100 °C, and forged at 450 °C. The basic properties of the TiO_2 powder for preparing the photocatalyst are listed in Table 2 [16]. The photocatalyst was finally ground into a powder. The reactant mixture of bioglycerol and acetic acid was poured into a three-necked round-bottom flask and catalyzed with the $\text{TiO}_2/\text{SO}_4^{2-}$ photocatalyst under ultraviolet light irradiation. The reaction time, reaction temperature, molar ratios, and photocatalyst's weight percentage of the glycerol were controlled to be 10 h, 120 °C, from 5 to 9, and 4 wt.%, respectively. The characteristics of the esterified product of glycerine acetate under various preparation conditions were analyzed to determine the optimum production conditions for the product. The glycerine acetate was used as an antifreeze for biodiesel.

The esterified product of bioglycerol obtained from the above procedures was mixed with the cosolvent and added to a commercial biodiesel made from waste cooking oil. The antifreeze mixture of 5 vol.% of the blended biodiesel was mixed with the biodiesel to improve its low-temperature fluidity. The fuel properties of the blended biodiesel, such as the cold filter plugging point (CFPP) and kinematic viscosity, were analyzed to evaluate the

effect of the antifreeze additive on the extent of fluidity enhancement of the glycerine acetate product to develop the economic value of the glycerol by-product of biodiesel production.

Table 1. Physical properties of glycerol [15].

Physical Properties	Glycerol
Chemical formula	C ₃ H ₈ O ₃
Boiling point (°C)	290
Melting point (°C)	17.9
Density (g/cm ³)	1.26
Absolute viscosity (Pa·s)	1.5
Flash point (°C)	160

Table 2. Basic properties of TiO₂ [16].

Physical Properties	TiO ₂
Average surface area (m ² /g)	124.7
Specific primary particle size (nm)	50.5
pH value in 4% dispersion	3.5–4.5
TiO ₂ content (%)	>99.5
Al ₂ O ₃ content (%)	<0.3
HCL content (%)	<0.3

2.2. Analysis of Fuel Characteristics of Blended Biodiesel

A volumetric moisture titrator (model DL-31, Mettler-Toledo Ltd., Greifensee, Switzerland) was used to measure the moisture content in the fuel sample within the range of 50 µg to 500 mg. The sample's moisture content in units of %, ppm, and mg was calculated automatically according to the amount of titrant consumed. An acid-value titrator (model 785DMP Titrino, Metrohm Ltd., Herisau, Switzerland) was used to measure the acid value of the fuel sample for a pH value ±20.0 and current measurement range ±200.0 µA. The electrode was selected based on the ion type. The standard solution was automatically added through the burette (models 765 and 776). The electrode head was activated by soaking it in deionized water for 60 s before use. The acid value of the sample was calculated automatically by injecting the sample into the instrument based on the consumed titrant using the built-in calculating formulas for acid values.

A manual tester of the cold filter plugging point (Hongsheng Science & Technology Ltd., Taoyuan City, Taiwan) was accompanied by a low-temperature circulating water tank (model B10/-40, Firstek Ltd., New Taipei City, Taiwan) to measure the cold filter plugging point (CFPP) of the fuel sample according to the test standards of CNS15061 and ASTM D6371. The test equipment measures CFPPs as low as -34 ± 0.5 °C. An elemental analyzer (model Vario EL III, Elementar Ltd., Langenselbold, Germany) was used to analyze the elementary compositions of the tested sample, including the chemicals, polymers, petrochemicals, soils, rubber, river sediments, etc. The weight percentages of nitrogen, hydrogen, carbon, oxygen, and sulfur in various non-explosive organic compounds in solid or liquid form were determined.

The constant water bath and fuel sample temperature reached 40 °C before the viscosity measurement, based on the ASTM D975-23 standard [17]. The kinematic viscosity of the fuel was measured using a viscosity test tube (model K69, Cannon Ltd., Coquitlam, BC, Canada) according to the DIN51562 formula, as shown below:

$$\nu = k \times t \quad (1)$$

where $k = 0.01045 \text{ mm}^2/\text{s}^2$ is the constant of the kinematic viscosity. The time lapse (t) for the fuel sample flowing between the indicated points on the test tube was recorded. The multiplication of k with t is the measured kinematic viscosity.

The heating value of the oil was measured by an oxygen bomb calorimeter (model 6200, Parr Ltd., Moline, IL, USA). Both solid and liquid samples were calculated based on the amount of heating energy released from the sample fuel to the water bath. A distillation temperature analyzer (Model HAD-620, Walter Herzog Ltd., Lauda-Königshofe, Germany) was used to measure the distribution of the distillation temperature of the fuel sample. T_{IBP} , T_{10} , T_{50} , and T_{EP} denote the temperatures corresponding to the initial water drop, 10 vol.%, 50 vol.%, and the last drop, respectively, of the fuel sample, which were distilled, condensed, and collected in the beaker on the other side. The specific gravity and distillation temperature were required to calculate the cetane index. The specific gravity was first converted to the API specific gravity G , and the distillation temperatures T_{IBP} and T_{50} were converted from $^{\circ}\text{C}$ to $^{\circ}\text{F}$ and applied to the cetane index (CI) calculation formula, as follows [18]:

$$G = 141.5/\text{sg} - 131.5 \quad (2)$$

$$\text{CI} = 0.016G^2 - 420.34 + 0.192G(\log T_{50}) + 65.01(\log T_{50})^2 - 0.0001809T_{50}^2 \quad (3)$$

where sg is the specific gravity, and T_{50} is the distillation temperature corresponding to 50 vol.% of the distilled and condensed fuel sample. The temperature used in Equation (3) is expressed in degrees Fahrenheit.

3. Results and Discussion

3.1. Effect of Irradiated UV Light and Molar Ratio on Fuel Characteristics of Glycerine Acetate

3.1.1. Effect of Irradiated UV Light and Molar Ratio on Freezing Point of Glycerine Acetate

The physical properties, including the molecular weight, boiling point, flash point, cold filter plugging point (CFPP), and specific gravity of the triacylglycerols (TAGs), diacylglycerols (DAGs), and monoacylglycerols (MAGs), are compared in Table 3 [19,20]. The TAG compound had the lowest freezing point (-78°C), while the MAG had the highest freezing point (18°C). The effects of the molar ratio of acetic acid/glycerol and UV-light irradiation on the $\text{TiO}_2/\text{SO}_4^{2-}$ photocatalyst surface on the freezing point of glycerine acetate is shown in Figure 1. The converted glycerine acetate under the irradiation of UV light appeared to have a significantly lower freezing point than that without UV-light irradiation, as shown in Figure 1. In addition, the freezing point decreased with the increase in the acetic acid/glycerol molar ratio.

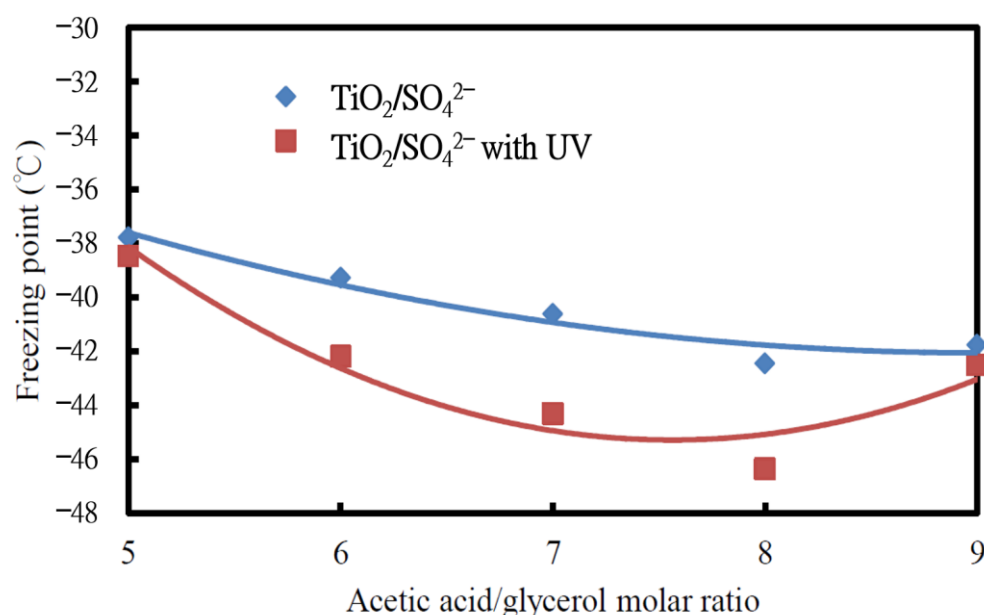


Figure 1. Effects of irradiation of ultraviolet (UV) light and acetic acid/glycerol molar ratio on the product's freezing point ($^{\circ}\text{C}$).

Table 3. Physical properties of TAGs, DAGs, and MAGs [19,20].

Physical Properties	Triacylglycerols (TAGs)	Diacylglycerols (DAGs)	Monoacylglycerols (MAGs)
Molecular weight (g/mol)	218.78	176.17	134.13
Boiling point (°C)	260	280	258
Flash point (°C)	142	140	145
Freezing point (°C)	−78	−30	18
Specific gravity (at 25 °C)	1.158	1.187	1.21

Increasing the molar ratio and UV light irradiation accelerates the glycerol conversion rate to form TAG, DAG, and MAG [21]. Hence, a higher molar ratio of acetic acid/glycerol and UV-light irradiation resulted in a larger TAG and lower MAG composition. Consequently, the freezing point of the glycerine acetate decreased with the increase in the molar ratio and UV-light irradiation because of the lowest freezing point of TAG. The lowest freezing point was observed at the molar ratio of acetic acid/glycerol equal to 8. A molar ratio of acetic acid/glycerol higher than 8 may retard the dehydration condensation reaction between -COOH radicals in the acetic acid molecules and OH[−] radicals in diacylglycerol (DAG) to produce a reverse reaction [22], resulting in lower TAG formation, and thus, a higher freezing point at a molar ratio of 9. Lin and Chen [23] also found that the TAG formation decreased from the highest amount of 40.41% to 34.63% when the molar ratio of acetic acid/glycerol increased from 8 to 9. Under UV irradiation on the solid-state strong acid photocatalyst surface, the photocatalyst will form an electron–electron hole pair. When the electron hole attaches to the water molecule, H⁺ and OH[−] will be generated. Under UV-light irradiation, acetic acid is prone to receiving H⁺ to accelerate the conversion reaction of glycerol. Therefore, the amount of glyceryl triacetate produced under UV-light irradiation is significantly higher than that produced without UV-light irradiation, as shown in Figure 1.

3.1.2. Effect of UV-Light Irradiation and Molar Ratio on Compositions of Glycerine Acetate

According to the above experimental results, a higher glycerol conversion rate and higher formation of triacylglycerols existed at the molar ratio of 8. The conversion reaction time, reaction temperature, and amount of added photocatalyst were 10 h, 120 °C, and 4 wt.% of glycerol, respectively. To irradiate the photocatalyst, UV light with a wavelength of 365 nm and power of 200 mW was used. As shown in Figure 2, the difference in the glycerol conversion rate between those with and without UV-light irradiation was insignificant. This is probably because, after 10 h of reaction time, the conversion process from glycerol to MAG, DAG, and TAG was almost complete. Under the UV-light irradiation with 200 mW power, triacylglycerols and diacylglycerols formed up to 55.17% and 33.54%, respectively, higher than those without the UV-light irradiation. However, the formation of monoacylglycerols under the UV-light irradiation was lower than that without the light irradiation because the UV-light irradiation facilitated the conversion from MAG to DAG and TAG [24] in turn, leading to a lower monoacylglycerol content in Figure 2.

Glycerine acetate was formed through the esterification reaction between glycerol and acetic acid, assisted by the irradiation of the photocatalyst by UV light with 200 mW power. The acetic acid receives H⁺ and reacts with the glycerol during the reaction process. A dehydration condensation reaction continues in the esterification process [25], leading to water formation. Triacylglycerols are the final product of the reaction process. The UV-light irradiation on the TiO₂/SO₄^{2−} solid-state strong acid photocatalyst surface enhanced the esterification reaction to form an electron–electron hole pair. When the electron hole attaches to the nearby water molecules, the oxidation process splits the water into H⁺ and OH[−]. Under the reaction environment, UV light irradiation will stimulate an even more significant amount of H⁺ [26], making the acetic acid easily accept H⁺ to react readily with the glycerol, accelerating the rate of the esterification reaction. Consequently, more triacylglycerols and diacylglycerols are produced under the photocatalytic effects.

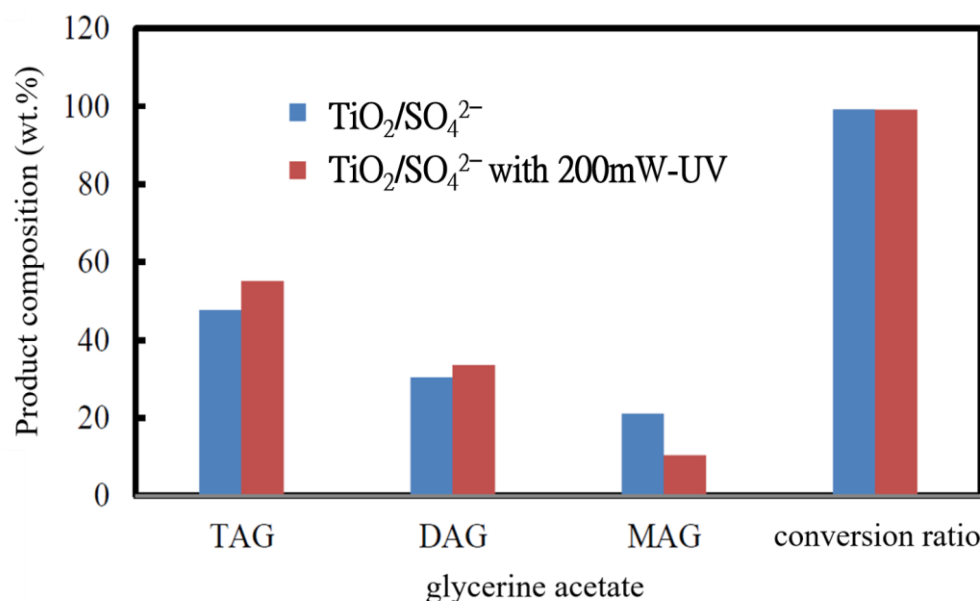


Figure 2. Comparison of product compositions and conversion ratio for the photocatalyst with and without UV-light irradiation.

3.2. Analysis of Fuel Properties

In this experiment, glycerine acetate was used as an antifreeze agent to improve the low-temperature fluidity of biodiesel fuel. Among various compounds of glycerine acetate, triacylglycerols (TAG) have the lowest cold filter plugging point (CFPP). Therefore, the higher the weight percentage of triacylglycerols (TAGs) in the product from the glycerol conversion, the more superior the fluidity enhancement of the antifreeze.

Antifreeze with superior CFPP characteristics was obtained from the glycerol conversion with acetic acid, which was assisted by UV-light irradiation on the TiO₂/SO₄²⁻ photocatalyst surface. The esterification reaction was carried out when the conditions of the reaction time, acetic acid/glycerol molar ratio, UV-light irradiation power, reaction temperature, and amount of the solid-state strong-acid photocatalyst were set to 10 h, 8, 200 mW, 120 °C, and 4 wt.% of the reacted glycerol, respectively. The mixture of the antifreeze product and a cosolvent of either methanol or butanol was then added to the biodiesel. The fuel properties of the blended biodiesel are analyzed and discussed below.

3.2.1. Kinematic Viscosity

Methanol or butanol was used as a cosolvent to be added to the antifreeze of glycerine acetate. The antifreeze and cosolvent mixture were then blended with the biodiesel at various weight percentages. The properties of the cosolvents of methanol and butanol and the antifreeze additive of glycerine acetate are compared in Table 4. The kinematic viscosities of methanol, butanol, and glycerine acetate were 0.58 mm²/s, 2.20 mm²/s, and 5.15 mm²/s, respectively, as shown in Table 4. In addition, methanol was observed to have the lowest specific gravity, flash point, and heating value among the three compounds [27]. The fuel properties of the neat biodiesel and the biodiesel with added 5 vol.% glycerine acetate are compared in Table 5. The addition of the antifreeze of glycerine acetate to the biodiesel was found to have slightly higher specific gravity and kinematic viscosity but a lower heating value, acid value, and cold filter plugging point (CFPP) than the neat biodiesel. The effects of the cosolvent, either methanol or butanol, and the volumetric ratio of the cosolvent to the antifreeze of glycerine acetate on the fuel properties, including the kinematic viscosity, carbon residue, acid value, cetane index, and CFPP, are illustrated in Figures 3–7. An increase in the volumetric ratio of the cosolvent/antifreeze was observed to decrease the kinematic viscosity in both cases of adding the methanol and butanol cosolvents. Methanol decreased the kinematic viscosity more significantly than butanol, as

shown in Figure 3. This is ascribed to the lower kinematic viscosity of methanol compared to butanol, as shown in Table 4. A significant decrease in the kinematic viscosity with the increase in the volumetric ratio of the butanol cosolvent was also found due to the most viscous property of glycerine acetate among the three compounds, as shown in Table 4, which reached 5.15 mm²/s.

Table 4. Physical properties of cosolvents and antifreeze of glycerine acetate [27].

Physical Properties	Butanol	Methanol	Glycerine Acetate
Specific gravity (at 15 °C)	0.81	0.79	1.16
Kinematic viscosity (mm ² /s, at 40 °C)	2.2	0.58	5.15
Flash point (°C)	35	12	140
Heating value (MJ/kg)	34.47	13.93	17.02

Table 5. Physical properties of neat biodiesel and biodiesel blended with antifreeze.

Physical Properties	Neat Biodiesel	Biodiesel with 5 vol.% Glycerine Acetate
Specific gravity (at 15 °C)	0.876	0.882
Kinematic viscosity (mm ² /s, at 40 °C)	4.281	4.290
Heating value (MJ/kg)	40.81	39.62
Acid value (mg KOH/g)	0.382	0.375
CFPP (°C)	3	2

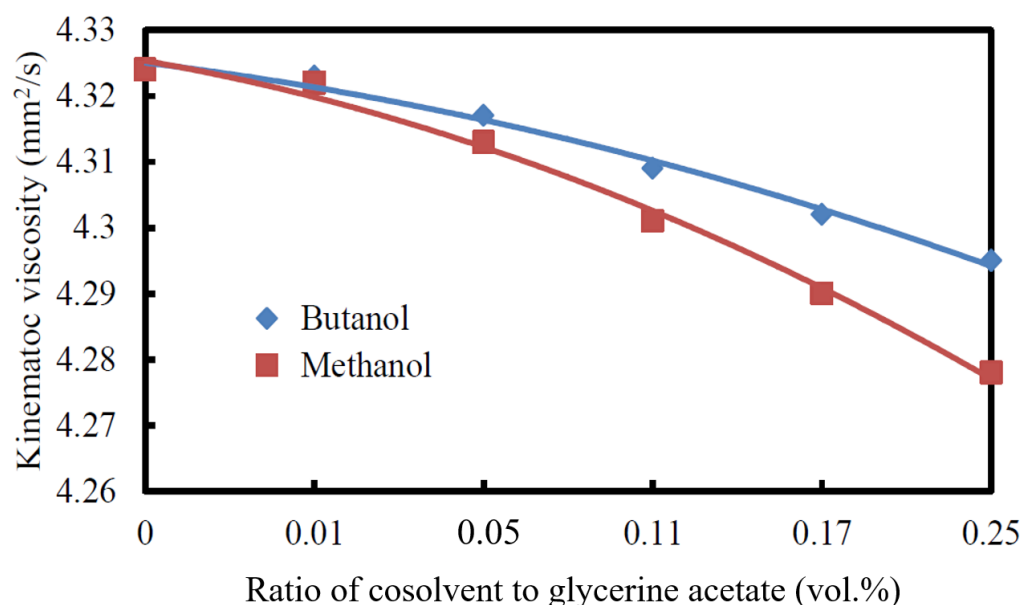


Figure 3. Effects of cosolvent and volumetric ratio of cosolvent to glycerine acetate on kinematic viscosity of blended biodiesel.

3.2.2. Heating Value

In this experiment, the heating value of the neat biodiesel before adding the antifreeze was 40.81 MJ/kg, which decreased to 39.62 MJ/kg after 5 vol.% glycerine acetates and cosolvent mixture of biodiesel was added to the biodiesel, as shown in Table 5. The heating values of the glycerine acetate, butanol, and methanol were 17.02 MJ/kg, 34.47 MJ/kg, and 13.93 MJ/kg, respectively, as shown in Table 4. The heating value of butanol was about two times that of glycerine acetate, while the heating value of methanol was the lowest, as shown in Table 4. The effects of the cosolvent type and volumetric ratio of the cosolvent/glycerine acetate on the heating value can be observed in Figure 4. The trends of the variations in the heating value with the volumetric ratio of the cosolvent/glycerine acetate for butanol and

methanol are different. An increase in the heating value with the increase in the volumetric ratio of butanol to glycerine acetate was found, which is in contrast to the slight decrease in the heating value with the increase in the volumetric ratio of methanol to glycerine acetate. A lower heating value indicates that a more significant fuel consumption rate is required to achieve the same power output, which is not favorable [28]. Therefore, the lower heating value of adding the cosolvent methanol implies a decrease in the combined heating value of the blended biodiesel with the increase in the volumetric ratio of methanol/antifreeze of glycerine acetate. In contrast, the increase in the volumetric ratio of butanol to glycerine acetate resulted in an increasing heating value of the blended biodiesel.

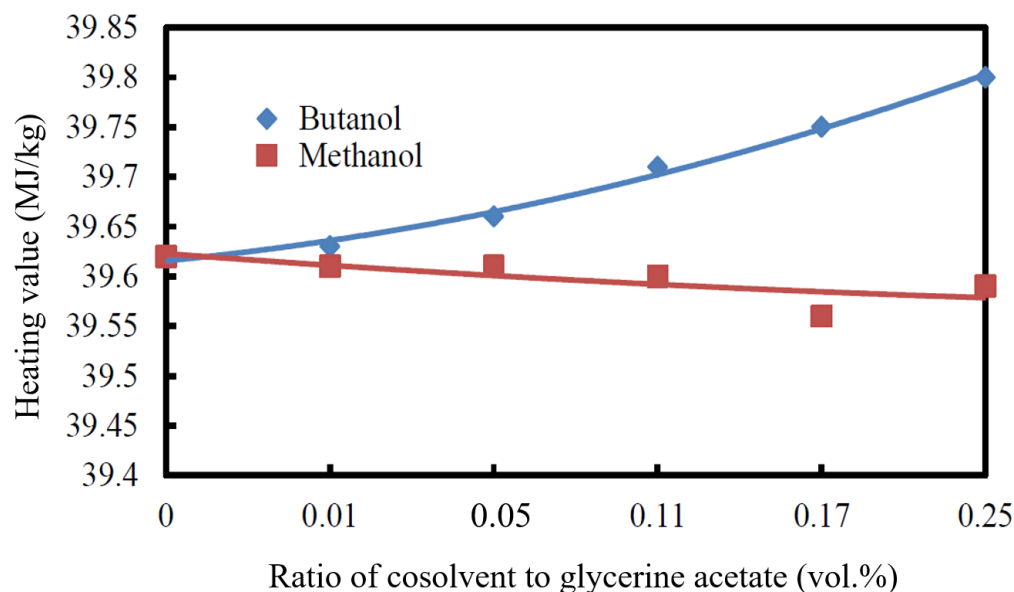


Figure 4. Effects of cosolvent and volumetric ratio of cosolvent to glycerine acetate on the heating value of the blended biodiesel.

3.2.3. Acid Value

Free fatty acid is produced from the hydrolysis reaction between fatty acid methyl esters and water, increasing biodiesel's acid value [29]. Water in the hydrolysis reaction divides the reacted compound into two parts. Hydrogen atoms in water are added to one part, while hydroxyl atoms are added to the other, forming two or more chemical compounds [30]. It is shown in Figure 5 that the higher the volumetric ratio of cosolvent/glycerine acetate, the higher the acid value of the blended biodiesel. The biodiesel blended with the cosolvent methanol was observed to have a higher acid value than that with butanol.

The acid value of the neat biodiesel increased from 0.427 mg KOH/g, without adding any cosolvent, to 0.810 mg KOH/g after the mixture of 0.25 vol.% methanol cosolvent and glycerine acetate was added to the biodiesel. The acid value of the biodiesel with the same amount of the mix of butanol cosolvent and glycerine acetate added reached a lower acid value of 0.770 mg KOH/g. This may be because the water content in the blended biodiesel promoted the hydrolysis reaction of either the methanol or butanol and fatty acid methyl esters to form free fatty acids. The hydrolysis reaction then caused an increase in the acid value. The rise in either methanol or butanol or, equivalently, the growth of the volumetric ratio of the cosolvent to glycerine acetate, facilitated the formation of free fatty acids, leading to an increase in the acid value of the blended biodiesel. Methanol is more prone to accelerate the hydrolysis reaction than butanol due to its relatively more straightforward structure of hydroxyl atoms [31], leading to an obviously higher acid value for the volumetric ratio of methanol/glycerine acetate from 0 to 0.25 vol.%.

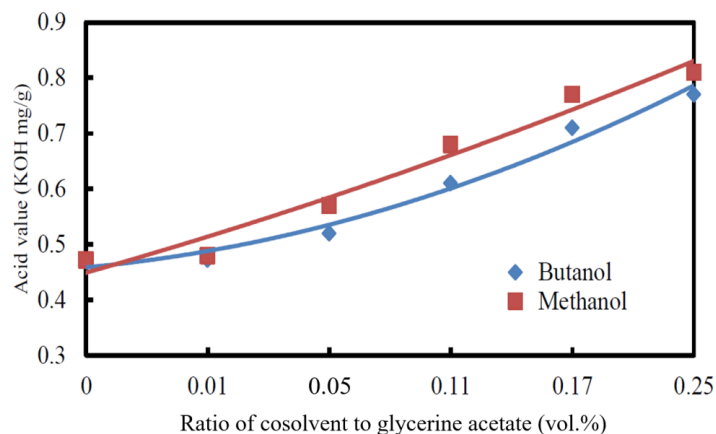


Figure 5. Effects of cosolvent and volumetric ratio of cosolvent to glycerine acetate on the acid value of the blended biodiesel.

3.2.4. Cetane Index

The cetane index is calculated based on the API gravity and the distillation temperature, at which 50% liquid fuel is vaporized, condensed, and collected after the distillation process, denoted as T_{50} [32]. The cetane index is an alternative indicator to the cetane number, which indicates the difficulty of compression-ignition of liquid fuel in a diesel engine. It was observed that only the distillation temperature of initial boiling (T_{IBP}) was changed significantly after adding different proportions of cosolvent/glycerine acetate to the biodiesel among various distillation temperatures from T_{IBP} to the end point of the distillation (i.e., T_{EP}) of the blended biodiesel. The T_{IBP} distillation temperature was found to decrease with the increase in the volumetric proportion of cosolvent/glycerine acetate because of the relatively lower boiling points of methanol and butanol, which are 46.7 °C and 114 °C, respectively, compared to 260 °C for TAG, as shown in Table 3. The effects of the cosolvent type and the volumetric ratio of cosolvent/glycerine acetate on the cetane index of the blended biodiesel are shown in Figure 6. The cetane index increased with the amount of cosolvent, particularly for the cosolvent methanol at volumetric ratios of cosolvent/glycerine acetate larger than 0.11. The addition of the cosolvent methanol was found to increase the cetane index more significantly than butanol. When methanol was used, the highest cetane index reached 47.25 at the 0.21 vol.% cosolvent of glycerine acetate. The cetane index of the blended biodiesel with the added cosolvent methanol was higher than that with butanol primarily because of the higher heating value and viscosity but lower volatility of the latter cosolvent [33]. Therefore, the increase in the volumetric ratio of the cosolvent/glycerine acetate facilitated the compression-ignition of the blended biodiesel.

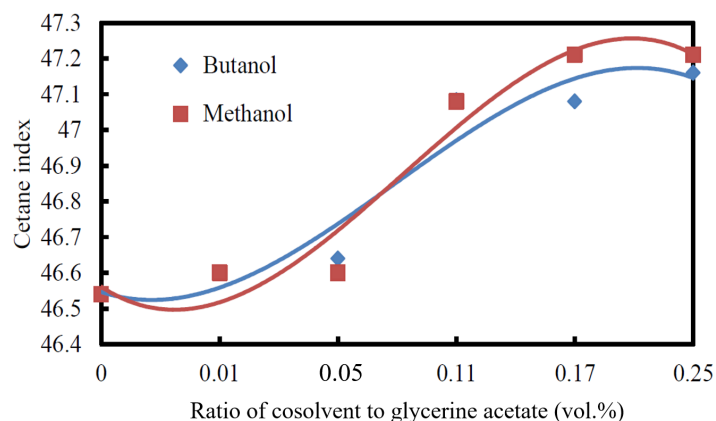


Figure 6. Effects of cosolvent and volumetric ratio of cosolvent to glycerine acetate on cetane index of the blended biodiesel.

3.2.5. Cold Filter Plugging Point

As shown in Table 5, the neat biodiesel's cold filter plugging point (CFPP) was 3 °C. Adding 5 vol.% glycerine acetate to the biodiesel only decreased the CFPP by 1 °C to 2 °C due to the high insolubility of glycerine acetate with fatty acid methyl esters. The anti-freezing effect of glycerine acetate was improved significantly by adding methanol or butanol as a cosolvent. When methanol was used as the cosolvent, the anti-freezing effect was obviously enhanced; specifically, when the volumetric ratio of the methanol cosolvent to glycerine acetate was 0.25 vol.%, the cold filter plugging point of the blended biodiesel was reduced from 3 °C to −2 °C after adding the mixture of cosolvent and antifreeze, as shown in Figure 7. In contrast, when the same amount of the butanol cosolvent and glycerine acetate mixture was added to the biodiesel, the cold filter plugging point of the biodiesel was only reduced from 3 °C to 1 °C. Laza and Bereczky [34] found that increases in the concentration of alcohols, such as butanol, ethanol, and methanol, in biodiesel reduced the CFPP of the fuel. In addition, there was no apparent CFPP reduction with the increase in the volumetric ratio of butanol to the antifreeze of glycerine acetate, as shown in Figure 7. Therefore, the optimum antifreeze mixture composition added to the biodiesel was 0.25 vol.% methanol cosolvent with glycerine acetate.

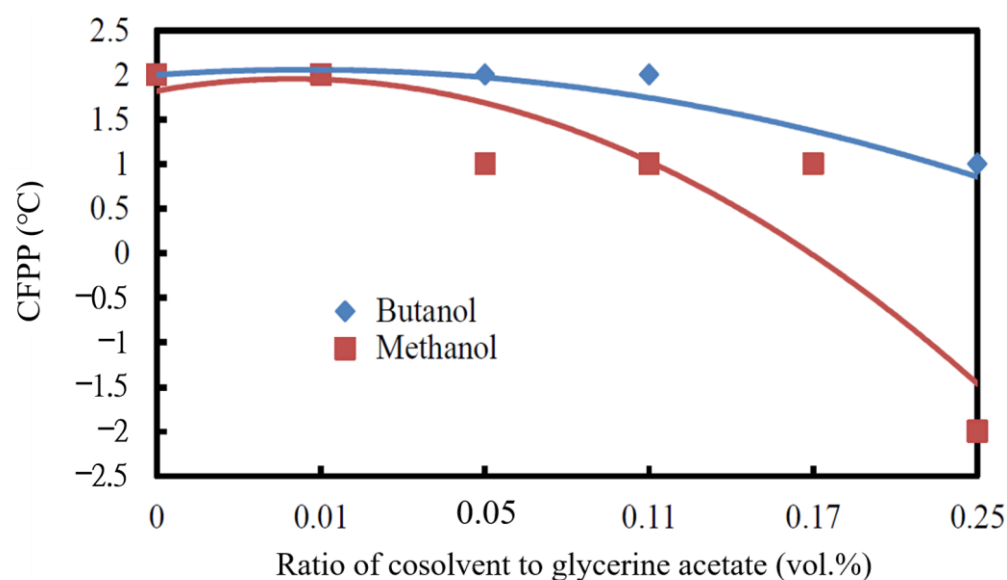


Figure 7. Effects of cosolvent and volumetric ratio of cosolvent to glycerine acetate on CFPP of the blended biodiesel.

4. Conclusions

- (1) The antifreeze of glycerine acetate, which was produced from the reactant mixture of acetic acid/glycerol at a molar ratio of 8 under UV-light irradiation, appeared to have the lowest freezing point, −46.36 °C. The UV-light irradiation on the $\text{TiO}_2/\text{SO}_4^{2-}$ photocatalyst surface rendered higher diacylglycerol (DAG) and triacylglycerol (TAG) but lower monoacylglycerol (MAG) production than those without UV-light irradiation.
- (2) The lowest cold filter plugging point (CFPP) was observed when the mixture of 0.25 vol.% methanol/antifreeze of glycerine acetate was added to the biodiesel, which decreased from 3 °C of the neat biodiesel to −2 °C of the blended biodiesel. The CFPP of the blended biodiesel only decreased to 1 °C if the cosolvent butanol was used instead.
- (3) The kinematic viscosity and CFPP decreased while the cetane index and acid value increased with the increase in the volumetric ratio of cosolvent/glycerine acetate added to the biodiesel.
- (4) The increase in the volumetric ratio of cosolvent/glycerine acetate increased the heating value of butanol while decreasing that of methanol for the blended biodiesel.

- (5) The cosolvent butanol in the blended biodiesel caused a higher CFPP, kinematic viscosity, and heating value but a lower acid value and cetane index than the cosolvent methanol.

Author Contributions: Formal analysis, C.-Y.L. and Y.-C.C.; methodology, C.-Y.L.; conceptualization, C.-Y.L.; investigation, C.-Y.L. and Y.-C.C.; data curation, Y.-C.C.; writing—original draft preparation, C.-Y.L. and Y.-C.C.; writing—review and editing, C.-Y.L.; supervision, C.-Y.L.; project administration, C.-Y.L. All authors have read and agreed to the published version of the manuscript.

Funding: This research was funded by the National Science and Technology Council, Taiwan, under contract number NSTC 109-2221-E-019-024.

Data Availability Statement: The data presented in this study are contained within this article.

Acknowledgments: The authors would like to gratefully acknowledge the financial support from the National Science and Technology Council, Taiwan, under contract number NSTC 109-2221-E-019-024.

Conflicts of Interest: The authors declare no conflicts of interest.

References

- Phung Hai, T.A.; Tessman, M.; Neelakantan, N.; Samoylov, A.A.; Ito, Y.; Rajput, B.S.; Pourahmady, N.; Burkart, M.D. Renewable Polyurethanes from Sustainable Biological Precursors. *Biomacromolecules* **2021**, *22*, 1770–1794. [CrossRef]
- Koul, R.; Kumar, N.; Singh, R.C. A review on the production and physicochemical properties of renewable diesel and its comparison with biodiesel. *Energy Sources A Recovery Util. Environ. Eff.* **2021**, *43*, 2235–2255. [CrossRef]
- Babamohammadi, S.; Yusoff, R.; Aroua, M.K.; Borhani, T.N. Mass transfer coefficients of carbon dioxide in aqueous blends of monoethanolamine and glycerol using wetted-wall column. *J. Environ. Chem. Eng.* **2021**, *9*, 106618. [CrossRef]
- Dhabhai, R.; Koranian, P.; Huang, Q.; Scheibelhoffer, D.S.B.; Dalai, A.K. Purification of glycerol and its conversion to value-added chemicals: A review. *Sep. Sci. Technol.* **2023**, *58*, 1383–1402. [CrossRef]
- Ioannidou, G.; Loukia Yfanti, V.; Lemonidou, A.A. Optimization of reaction conditions for hydrodeoxygenation of bio-glycerol towards green propylene over molybdenum-based catalyst. *Catal. Today* **2023**, *423*, 113902. [CrossRef]
- Lima, P.J.M.; da Silva, R.M.; Neto, C.A.C.G.; Gomes e Silva, N.C.; Souza, J.E.d.S.; Nunes, Y.L.; Sousa dos Santos, J.C. An overview on the conversion of glycerol to value-added industrial products via chemical and biochemical routes. *Biotechnol. Appl. Biochem.* **2022**, *69*, 2794–2818. [CrossRef]
- Karawek, A.; Kittipoom, K.; Tansuthepverawongse, L.; Kitjanukit, N.; Neamsung, W.; Lertthanaphol, N.; Chanthara, P.; Ratchahat, S.; Phadungbut, P.; Kim-Lohsoontorn, P.; et al. The Photocatalytic Conversion of Carbon Dioxide to Fuels Using Titanium Dioxide Nanosheets/Graphene Oxide Heterostructure as Photocatalyst. *Nanomaterials* **2023**, *13*, 320. [CrossRef] [PubMed]
- Nivetha, N.; Thangamani, A.; Velmathi, S. Sulfated Titania (TiO₂-SO₄²⁻) as an Efficient Catalyst for Organic Synthesis: Overarching Review from 2000 to 2021. *ChemistrySelect* **2022**, *7*, e202104505. [CrossRef]
- Jin, R.; Li, G.; Sharma, S.; Li, Y.; Du, X. Toward Active-Site Tailoring in Heterogeneous Catalysis by Atomically Precise Metal Nanoclusters with Crystallographic Structures. *Chem. Rev.* **2021**, *121*, 567–648. [CrossRef]
- Mujtaba, M.A.; Kalam, M.A.; Masjuki, H.H.; Gul, M.; Soudagar, M.E.M.; Ong, H.C.; Ahmed, W.; Atabani, A.E.; Razzaq, L.; Yusoff, M. Comparative study of nanoparticles and alcoholic fuel additives-biodiesel-diesel blend for performance and emission improvements. *Fuel* **2020**, *279*, 118434. [CrossRef]
- Al-Rabiah, A.A.; Al Darwish, R.K.; Alqahtani, A.E.; Chaves, D.M.; da Silva, M.J. Production of Biofuel Additives Using Catalytic Bioglycerol Etherification: Kinetic Modelling and Reactive Distillation Design. *Catalysts* **2022**, *12*, 1332. [CrossRef]
- Matkala, B.; Boggala, S.; Basavaraju, S.; Sarma Akella, V.S.; Aytam, H.P. Influence of sulphonation on Al-MCM-41 catalyst for effective bio-glycerol conversion to Solketal. *Microporous Mesoporous Mater.* **2024**, *363*, 112830. [CrossRef]
- Hájek, M.; Vávra, A.; Mück, J. Butanol as a co-solvent for transesterification of rapeseed oil by methanol under homogeneous and heterogeneous catalyst. *Fuel* **2020**, *277*, 118239. [CrossRef]
- Yaman, H.; Yesilyurt, M.K.; Shah, R.M.R.A.; Soyhan, H.S. Effects of compression ratio on thermodynamic and sustainability parameters of a diesel engine fueled with methanol/diesel fuel blends containing 1-pentanol as a co-solvent. *Fuel* **2024**, *357*, 129929. [CrossRef]
- Perry, R.H.; Green, D.W. *Perry's Chemical Engineer's Handbook*, 9th ed.; McGraw Hill: New York, NY, USA, 2018.
- Uni-Onward Corp. *TiO₂ Property Manual*; Uni-Onward Corp: New Taipei City, Taiwan, 2020.
- ASTM D975-23; Standard Specification for Diesel Fuel. ASTM International: West Conshohocken, PA, USA, 2023. Available online: <https://cdn.standards.iteh.ai/samples/116070/362c5db72e9d452da0eddf0c5a056dc0/ASTM-D975-23.pdf> (accessed on 7 April 2023).
- Lin, C.-Y.; Wu, X.-E. Determination of Cetane Number from Fatty Acid Compositions and Structures of Biodiesel. *Processes* **2022**, *10*, 1502. [CrossRef]
- Aktas, A.B.; Ozen, B.; Alamprese, C. Effects of processing parameters on chemical and physical properties of enzymatically interesterified beef tallow–corn oil blends. *J. Food Process. Preserv.* **2021**, *45*, e14587. [CrossRef]

20. Wang, X.; Ma, D.; Liu, Y.; Wang, Y.; Qiu, C.; Wang, Y. Physical properties of oleogels fabricated by the combination of diacylglycerols and monoacylglycerols. *J. Am. Oil Chem. Soc.* **2022**, *99*, 1007–1018. [[CrossRef](#)]
21. Oliveira, L.; Pereira, M.; Pacheli Heitman, A.; Filho, J.; Oliveira, C.; Ziolk, M. Niobium: The Focus on Catalytic Application in the Conversion of Biomass and Biomass Derivatives. *Molecules* **2023**, *28*, 1527. [[CrossRef](#)]
22. Tonutti, L.G.; Dalla Costa, B.O.; Decolatti, H.P.; Mendow, G.; Querini, C.A. Determination of kinetic constants for glycerol acetylation by particle swarm optimization algorithm. *Chem. Eng. J.* **2021**, *424*, 130408. [[CrossRef](#)]
23. Lin, C.Y.; Chen, Y.C. Effects of heterogeneous sulfated acid photocatalysts and irradiation of ultraviolet light on the chemical conversion and characteristics of antifreeze from bioglycerol. *Processes* **2024**, *12*, 383. [[CrossRef](#)]
24. Ahmed, M.T.; Farooqui, S.A.; Hsu, S.H.; Daeun, L.; Chaerun, S.K. Valorizing Glycerol into Valuable Chemicals through Photocatalytic Processes Utilizing Innovative Nano-Photocatalysts. In *Solar Light-to-Hydrogenated Organic Conversion: Heterogeneous Photocatalysts*; Springer Nature: Singapore, 2024; pp. 149–234.
25. Khan, Z.; Javed, F.; Shamair, Z.; Hafeez, A.; Fazal, T.; Aslam, A.; Zimmerman, W.B.; Rehman, F. Current developments in esterification reaction: A review on process and parameters. *J. Ind. Eng. Chem.* **2021**, *103*, 80–101. [[CrossRef](#)]
26. Arora, I.; Chawla, H.; Chandra, A.; Sagadevan, S.; Garg, S. Advances in the strategies for enhancing the photocatalytic activity of TiO₂: Conversion from UV-light active to visible-light active photocatalyst. *Inorg. Chem. Commun.* **2022**, *143*, 109700. [[CrossRef](#)]
27. Iliev, S. A Comparison of Ethanol, Methanol, and Butanol Blending with Gasoline and Its Effect on Engine Performance and Emissions Using Engine Simulation. *Processes* **2021**, *9*, 1322. [[CrossRef](#)]
28. Lin, C.-Y.; Lin, K.-H.; Yang, H. Effects of Surfactant Characteristics on Fuel Properties of Emulsions of Alternative Engine Fuel through the Phase Inversion Method. *Processes* **2023**, *11*, 1864. [[CrossRef](#)]
29. Ortiz Lechuga, E.G.; Rodríguez Zúñiga, M.; Arévalo Niño, K. Efficiency Evaluation on the Influence of Washing Methods for Biodiesel Produced from High Free Fatty Acid Waste Vegetable Oils through Selected Quality Parameters. *Energies* **2020**, *13*, 6328. [[CrossRef](#)]
30. Remucal, C.K.; Salhi, E.; Walpen, N.; von Gunten, U. Molecular-Level Transformation of Dissolved Organic Matter during Oxidation by Ozone and Hydroxyl Radical. *Environ. Sci. Technol.* **2020**, *54*, 10351–10360. [[CrossRef](#)]
31. Zhen, X.; Wang, Y.; Liu, D. Bio-butanol as a new generation of clean alternative fuel for SI (spark ignition) and CI (compression ignition) engines. *Renew. Energy* **2020**, *147*, 2494–2521. [[CrossRef](#)]
32. Lin, C.-Y.; Lin, K.-H. Comparison of the Engine Performance of Soybean Oil Biodiesel Emulsions Prepared by Phase Inversion Temperature and Mechanical Homogenization Methods. *Processes* **2023**, *11*, 907. [[CrossRef](#)]
33. Ning, L.; Duan, Q.; Chen, Z.; Kou, H.; Liu, B.; Yang, B.; Zeng, K. A comparative study on the combustion and emissions of a non-road common rail diesel engine fueled with primary alcohol fuels (methanol, ethanol, and n-butanol)/diesel dual fuel. *Fuel* **2020**, *266*, 117034. [[CrossRef](#)]
34. Laza, T.; Bereczky, Á. Basic fuel properties of rapeseed oil-higher alcohols blends. *Fuel* **2011**, *90*, 803–810. [[CrossRef](#)]

Disclaimer/Publisher's Note: The statements, opinions and data contained in all publications are solely those of the individual author(s) and contributor(s) and not of MDPI and/or the editor(s). MDPI and/or the editor(s) disclaim responsibility for any injury to people or property resulting from any ideas, methods, instructions or products referred to in the content.